Applied Acoustics 184 (2021) 108349

Contents lists available at ScienceDirect

Applied Acoustics

journal homepage: www.elsevier.com/locate/apacoust

Effect of tree species and season on the ability of forest floors to abate environmental noise

Timothy Van Renterghem [a,*], Floris Huyghe [a,b], Kris Verheyen [b]

[a] Ghent University, Department of Information Technology, WAVES Research Group, Technologiepark 126, B 9052 Gent-Zwijnaarde, Belgium
[b] Ghent University, Department of Environment, Forest & Nature Lab, Geraardsbergsesteenweg 267, B 9090 Melle-Gontrode, Belgium

ARTICLE INFO

Article history:
Received 19 March 2021
Received in revised form 31 July 2021
Accepted 5 August 2021

Keywords:
Outdoor sound propagation
Acoustic impedance
Outdoor soils
Forest floor
Vegetation

ABSTRACT

The nature of the ground beneath a belt of trees along transport infrastructure can contribute significantly to the associated noise abatement. To get more insight in this topic, repeated measurements were performed, both in winter and summer time, in a common garden of six monoculture broadleaved tree stands (ash, cherry, lime, maple, beech and oak, all of the same age). A two-microphone technique was used to derive the ground surface impedance and soil properties describing the interaction between the forest floor and sound waves. The slit-pore and Zwikker and Kosten (phenomenological) ground impedance model, both in rigid backing configuration, were found to adequately predict the measured short-range level differences. The much higher moisture content of the forest floor during the winter campaign resulted in a strong increase in the deduced surface impedance. A clear overall tree species effect seemed absent, despite large differences in litter degradation rates. Additional measurements after raking away the organic layer allowed concluding that a pronounced forest floor might compensate for an acoustically harder mineral soil beneath. In tree belts aiming at noise reduction, litter should not be removed and care is needed not to compact the mineral soil, especially in case of stands with rapidly decaying litter and a thin organic horizon.

1. Introduction

The nature of the ground surface formed in areas with significant tree coverage, henceforth called the "forest floor", contributes significantly to the noise abatement by tree belts or strips of forests along surface transport infrastructure. Compared to sound propagation over other types of (natural) grounds, a very pronounced and broad destructive interference is observed between the direct sound path and the ground reflected path [1]. In addition to the source-receiver geometry, this interference depends on the surface impedance of the ground which in turn is influenced strongly by its flow resistivity. When listing flow resistivities of outdoor soils, forest floors are usually ranked as second lowest after "freshly fallen snow" [2,3]. A major asset of this acoustical ground effect (often denoted as "ground dip") is that it occurs in the low frequency range for a typical source-receiver geometry, so at sound frequencies where other attenuation processes are limited. Atmospheric absorption, e.g., is negligible at low sound frequencies, and noise abatement measures relying on the diffraction principle (such as a traditional noise wall) perform poorly in the low frequency range. Exploiting this forest floor effect could thus be of special interest in reducing noise exposure near roads [1,4].

In contrast to the noise reduction provided by above ground biomass, the forest floor effect is since long seen as a robust effect [5–9]. Trunks will mainly lead to multiple scattering of sound, where the sound absorption by tree barks, although limited [10], is helpful [10]. But only when tree trunk density is close to its biological maximum [11] can significant effects be expected from the scattering process. The relative contributions of the forest floor effect and the trunks have been examined numerically for shallow tree belts in Ref. [11]. Under the condition of high tree trunk densities, and when the tree belt directly borders the road, both the scattering and ground effect are predicted to contribute more or less equally to the overall road traffic noise reduction. For more common and less dense tree belts, with smaller basal areas, the forest floor effect is expected to be the dominant process responsible for noise reduction.

* Corresponding author at: Ghent University, Department of Information Technology, WAVES Research Group, Technologiepark 126, B 9052 Gent-Zwijnaarde, Belgium.
E-mail address: timothy.vanrenterghem@ugent.be (T. Van Renterghem).

https://doi.org/10.1016/j.apacoust.2021.108349
0003-682X/

Despite their potential acoustical significance, extensive and systematic acoustic measurements of forest floors are lacking. Typical parameter ranges for a few forest floors can be found in related literature (see e.g. [1,12–14]). Engineering methods for outdoor sound propagation like NORD2000 [2] or CNOSSOS [3] provide flow resistivity ranges for a generic "forest floor". Little or no information is available regarding the effect of tree species. Species and stand characteristics, however, determine the properties of the forest floor [15]. Species could thus be a potentially interesting design parameter to optimize tree belts when planned for noise reduction.

Mature forest floors are multi-layered, consisting of a mineral layer, a humified layer, a fragmentation layer, and a litter layer with less decomposed material [12,15]. In layered porous media, in general, the underlying layers influence the surface impedance as encountered at the interface with the air [16]. Tree species and stand characteristics will influence the structure, thickness and composition of the various forest floor layers. The forest floor under tree species with good decomposing litter typically consists of a shallow litter layer and the absence of a fragmentation and humified layer (a so-called 'mull' humus form). By contrast, all three organic layers are found under tree species with a poor litter quality (a so-called 'mor' humus form). With all other factors equal (soil type, stand density, etc.), the mass of the organic forest layer under different tree species can vary by a factor 60, ranging from <1 ton per ha to more than 60 tons per ha [17]. To increase understanding of the acoustic forest floor effect, the relative contributions of these layers need research. Under the assumption that the organic layer is relevant for its acoustical effect, an important factor might be its decomposition rate. Therefore, in the current study, species with contrasting litter quality and degradation rate were selected. In addition, measurements were performed above the undisturbed forest floor, but also after manually removing the top organic forest floor layer at the same location. From research on building envelope greening, there is clear evidence that leaf-cover influences the surface impedance of growing substrates [18–20] and that the percentage of organic matter might be important [20].

The spatio-temporal variability of the forest floor effect is of interest as well. Short-range variations in the acoustical properties might lead to surface impedance variations, affecting sound waves propagating over it [1]. At a somewhat larger spatial scale, the homogeneity of the forest floor effect within a species stand is of interest as well. Grassland sites, e.g., are characterized by a remarkable variation in acoustic surface impedance [1], meaning that generalization might be difficult to acoustically describe this type of outdoor ground. The measurement campaign in this paper is designed to analyse both short- and longer-range spatial variability.

Temporal variations might be driven by season and by the changing forest floor moisture content. Just like for common outdoor soils, it can be expected that the acoustic impedance increases with increasing soil moisture content [21–25]. This can be attributed to various effects such as a reduced effective layer thickness of the porous ground medium, a decreased porosity by swelling of soil particles, and clogging of pores making it more difficult for sound waves to penetrate the soil. Even small amounts of water were shown to significantly influence the acoustic surface admittance of sandy soils [23]. Due to its physical characteristics (low bulk density, large pore space), the water holding capacity of the organic forest floor layer is high [26] and its moisture content in dry versus wet periods can vary with a factor ten (see e.g. [27]). To take such effects into account, measurements were made both during winter time (after a long period of intense rainfall) and during summer time (after a long dry period), at the same forest stands.

2. Materials and methods

2.1. Experimental site

The measurement campaigns took place in the 13 ha Mortagne forest (at about 10 km south-east of the city of Kortrijk, in the northwest of Belgium, at 50°46′14″N 3°21′46″E). There, 0.5 ha (or larger) monoculture plots of different deciduous tree species were planted on former agricultural land, all in 1971 (see Fig. 1). As a consequence, the forest floor is still developing and a (dynamic) forest floor biomass equilibrium has probably not been reached yet. In temperate forests this may take up to a century or more [28]. Nevertheless, such a developing forest floor is representative for many tree belts established along transport. The soil type in the entire forest is a Haplic Luvisol, with 10% clay, 40–60% silt and 30–50% sand on average (see Ref. [29] for more info). Six species (American white ash – *Fraxinus americana*, small-leaved lime – *Tilia cordata*, sweet cherry – *Prunus avium*, northern red oak – *Quercus rubra*, beech – *Fagus sylvatica*, and sycamore maple – *Acer pseudoplatanus*) were selected based on their contrasting leaf litter degradation properties. Beech and oak have the poorest litter quality, whereas ash and cherry have the highest. Lime and maple have intermediate values [29]. The build-up and thickness of the organic layer will therefore differ between these species. The Mortagne forest is located in a quiet agricultural environment (see Fig. 1), at more than 2 km from the nearest (national) road.

During the winter campaign (see Fig. 1), two locations were considered in each selected stand, while during the summer campaign, measurements were performed at three locations (except for plot 5c, due to lack of sufficient space to position the measurement frame – see further). The summer measurements were made as close as possible to the locations of the winter measurements, but not exactly at the same spot since the forest floor was disturbed due to handling of the loudspeaker-microphone containing structure and by removing the organic forest floor. In contrast to the measurements reported in Ref. [30], working on a single line in open field conditions, the locations were randomly selected in the more open parts of the plots, to allow placement of the structure and to avoid scattering by tree trunks at very close distance from either the microphone or the loudspeaker. Each measurement was repeated by rotating the experimental setup over 90° to get information regarding very short-range variability.

The winter measurements (February–March 2020) were performed after a period with intense rainfall when the soil was saturated with water. During the actual measurements there was no rain, and the average air temperature was about 10 °C. During the summer campaign (August 2020), measurements were done after a long dry and warm period, the average air temperature during the measurement days was 27 °C.

2.2. Measurement methodology and instrumentation

2.2.1. Short range spectral level difference measurements using the template method

Acoustical ground information was deduced by means of short range spectral level difference measurements at two microphones positioned on top of each other close to a loudspeaker. The source-receiver geometry was based on the NORDTEST methodology [31] and ANSI/ASA S1.18-2018 [32]; the center of the source and one of the microphones were at roughly 0.5 m above the ground. The lowest microphone was placed at a height of 0.2 m. The distance between source and receiver in our setup was about 1.75 m. Such a distance ensures that the loudspeaker could be considered as a point source for the range of frequencies considered, yet allowing a good signal-to-noise ratio at the microphones. Measurements

Fig. 1. Overview of the Mortagne forest showing its surroundings and the subdivision in monoculture forest stands. The dots indicate the measurement spots during the winter and summer campaign in the selected stands (American white ash – Fraxinus americana – 1a, small-leaved lime - Tilia cordata – 5a, sweet cherry - Prunus avium – 5c, northern red oak - Quercus rubra – 6a, beech - Fagus sylvatica – 6c, and sycamore maple - Acer pseudoplatanus – 8a).

were performed at the spectral detail of 1/3 octave bands. For each measurement, a second microphone height pair was considered as well, namely at 0.2 m and 0.75 m (with the source height still at 0.5 m).

Instead of directly trying to derive the impedance at each frequency band, a so-called ground impedance template method [1,14] was used. When combining a physically admissible surface impedance model and a 2-ray point source propagation model [1], the acoustical soil parameters can be reasonably well deduced by fitting on the measurements [1]. The derived soil parameters are then sometimes indicated as "effective" [14] parameters. This template method has the advantage of more consistent outcomes. In addition, it allows the parameters from the fitting to be directly used when the same ground impedance model is considered while calculating sound propagation in future applications. More detailed information on this non-destructive *in-situ* technique, together with an overview of alternative approaches, can be found in Ref. [1].

2.2.2. Instrumentation and signals

Not only the interactions between the sound waves and the ground, but also the relative positioning of loudspeaker and microphones define the level difference spectra of two vertically positioned microphones. To increase the sensitivity of the measurements to small differences in the *in-situ* acoustically determined soil parameters, it is important to ensure full control on the source and microphone positioning. Therefore, a metal frame was constructed (see Fig. 2a and b) which is easy to assemble/disassemble and that fixes the heights of the loudspeaker and microphones and their separation.

A square ground plane with sufficient side length (2 m, see Fig. 2a and b) was used to minimize interaction between sound waves scattering from parts of the frame lying on the ground and the specular reflection point located near its center. The microphones were slightly positioned off-center to prevent scattering by vertical supporting poles directly near the microphones. The tubes forming the frame have a diameter of 2.7 cm to ensure sufficient stability, but at the same time, keeping sound scattering limited.

Two ½ inch type-1 microphones (BK 4189) were used, each with a Svantek 12L preamplifier, connected to its own single-channel battery driven handheld sonometer (Svantek 959), allowing for 1/3 octave band analysis. Microphone calibration was performed with a Svantek SV30A type-1 94-dB calibrator. The loudspeaker was a commercially available battery driven bluetooth device (JBL flip 3). The size of the loudspeaker (i.e. a cylinder with a diameter of 6.4 cm and a length of 16.9 cm) is a compromise between providing sufficient output power, also at lower frequencies, while allowing that the speaker can still be represented as a point source to ease its modelling.

Time synchronization between the two measurement chains was not necessary; sufficiently long noise sequences were emitted, over which the spectral equivalent sound pressure levels were calculated. Each measurement consisted of 3 noise bursts of 20 s long of constant amplitude, followed by pauses each with a duration of 10 s (see Fig. 2c and d). Such a procedure allowed to check repeatability of the sound pressure level differences during the signal-on periods. The measured level difference spectra were linearly averaged afterwards. At the same time, three periods of background noise were measured in between to allow checking the signal-to-noise ratio. A level difference of 10 dB at any frequency band considered during the signal on period (relative to the signal off period) was obtained in almost all measurements (see Fig. 2e). One-third octave bands for which a signal-to-noise ratio of 10 dB was not reached were consequently disregarded during the fitting process.

2.2.3. Analytical point source model

A two-ray analytical model was used, commonly known as the "Weyl-Van der Pol model" [1], for sound propagation over locally-reacting smooth flat ground from a stationary point source in a homogeneous and non-moving atmosphere, in absence of atmospheric absorption. The sound pressure level difference between the high and the low microphone can be calculated as follows:

$$\Delta L_p = 20\log_{10}\left[\frac{\left|\frac{e^{ikR_{1,high}}}{R_{1,high}} + Q_{high}\frac{e^{ikR_{2,high}}}{R_{2,high}}\right|}{\left|\frac{e^{ikR_{1,low}}}{R_{1,low}} + Q_{low}\frac{e^{ikR_{2,low}}}{R_{2,low}}\right|}\right] \quad (1)$$

In this equation, k is the sound wave number in air, Q is the spherical wave pressure reflection coefficient at the ground plane, R_1 is the length of the direct sound path between the source and the receiver, and R_2 is the total distance travelled by the ground reflected wave (assuming specular reflection). The subscripts "low" and "high" stand for the parameters linked to the higher and lower positioned microphones.

The spherical reflection coefficient Q depends on the source-receiver geometry, the ground surface impedance Z_s and the wave number k. For a complete mathematical description and a set of formulae to calculate Q, the reader is referred to Chapter 2 in Ref. [1]. Note that this is a classical and widely used analytical sound propagation model, whose results are considered to be highly

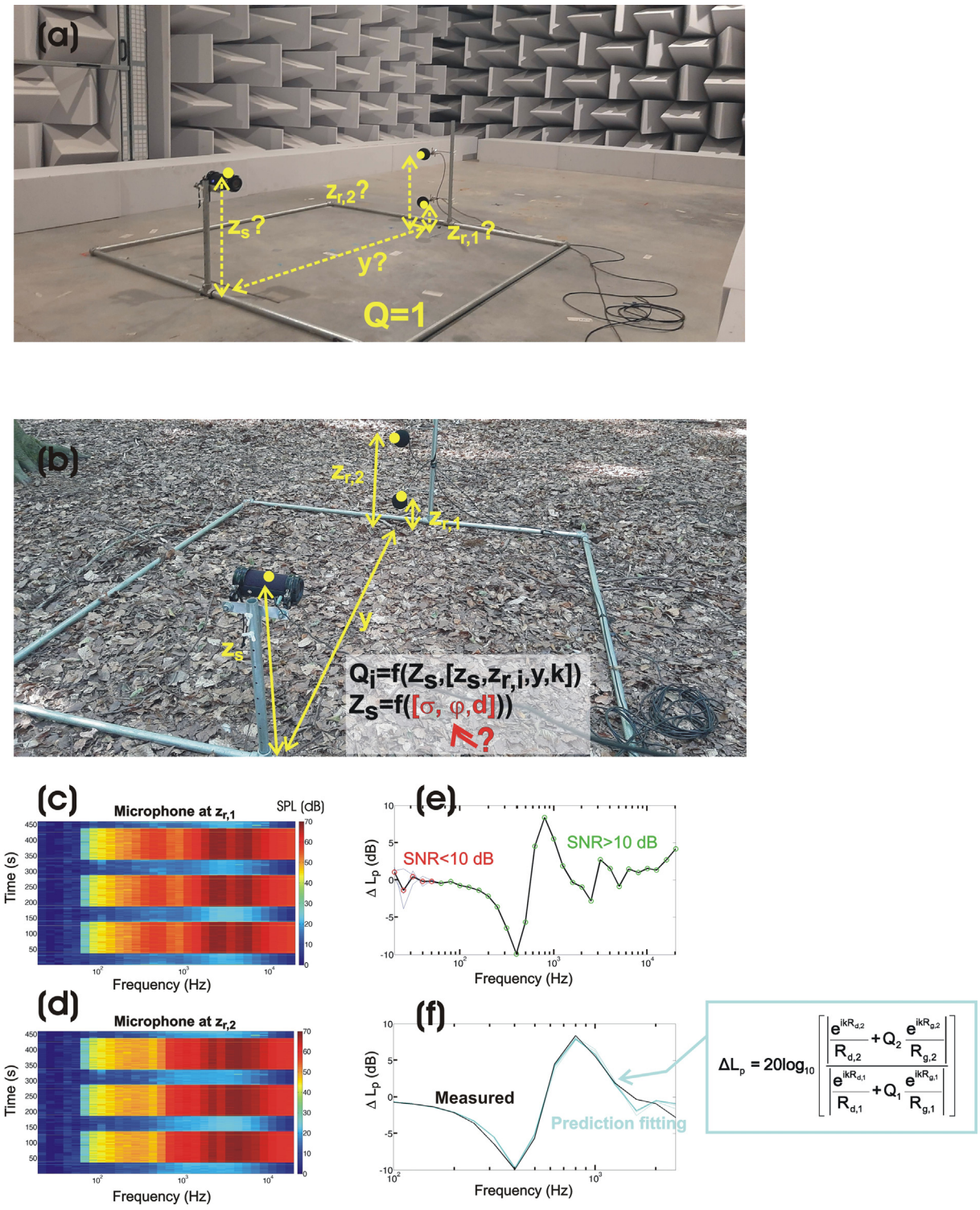

Fig. 2. Overview of the instrumentation, measurement procedure and signal processing to deduce the acoustic forest floor parameters. In (a), the optimization procedure to find the optimal point source/point receiver geometry in the semi-anechoic chamber is illustrated (see Appendix A); in (b), the frame containing the loudspeaker and microphones is shown, positioned in situ, with indication of the procedure to find the acoustical soil parameters; in (c) and (d), example measured spectrograms of the signal played, captured at the lower (c) and higher (d) positioned microphones, are shown; in (e), the measured level difference spectra between the microphones are plotted with indication whether a 1/3 octave band has a sufficient signal-to-noise (SNR) ratio; in (f), the best fit on the level difference measurements for this specific situation is shown. The processing of a single microphone pair is shown, for a measurement of the undisturbed forest floor. In these figures, source height is indicated by z_s, the ground projected source-receiver separation by y, and the lower and upper microphone heights by $z_{r,1}$ and $z_{r,2}$. The other symbols are explained in Sections 2.2.3 and 2.2.4.

accurate [1]. The simulated sound pressure level differences were aggregated to 1/3 octave bands, similar to the measurement results.

2.2.4. Ground impedance models

Two candidate ground impedance models were selected that showed reasonably accurate fits on short-range spectral level

difference data for a wide range of natural grounds [14]. The choice here will be limited to ground impedance models with three parameters or less, as these are most widely used. Note that forest floors, due to their layering, might behave in a (more) complex way. However, more advanced ground impedance models (see Ref. [1] for an overview) might be less suited for the parameter deduction approach followed in this work, potentially leading to overfitting or fitted parameters with a non-physical meaning.

The three-parameter Zwikker and Kosten (ZK) phenomenological model [33] is of interest since it allows an easy implementation in time-domain acoustic models [34]. The specific characteristic impedance $Z_{c,ZK}$ (relative to the impedance of air) and the wave number k_{ZK} read:

$$q_c = \left(\frac{k_s}{\varphi}\right) + i\left(\frac{\sigma}{2\pi f \rho_{air}}\right) \tag{2}$$

$$Z_{c,ZK} = \sqrt{\frac{q_c}{\varphi}} \tag{3}$$

$$k_{ZK} = \left(\frac{2\pi f}{c}\right)\sqrt{q_c \varphi} \tag{4}$$

with k_s the structure constant (which is parameter similar to the tortuosity), φ the porosity of the ground medium, σ the flow resistivity, f the sound frequency, ρ_{air} the mass density of air, c the sound speed in (unbounded) air and i the imaginary unit.

In this work, a two-parameter version of the ZK model was used, assuming a fixed relationship between the structure factor and the porosity, namely:

$$k_s = \sqrt{\frac{1}{\varphi}} \tag{5}$$

This simplification expressed by Eq. (5) limits the degrees of freedom during the fitting process, see Ref. [14] for a detailed discussion on this.

The slit-pore model (SP) [35,36] is a two-parameter rigid-porous approach, characterized by a complex density, linked to viscous effects, and a complex compressibility, linked to thermal processes. Various forms of these complex quantities can be obtained by assuming ideally shaped pores in the ground medium, such as slits. This offers a more rigorous basis for ground surface impedance models [1]. The characteristic normalized impedance $Z_{c,SP}$ and slit-pore wave number k_{SP} are:

$$Z_{c,SP} = \frac{1}{c\rho_{air}}\sqrt{\left(\frac{T}{\varphi^2}\right)\frac{\rho(\lambda)}{C(\lambda)}} \tag{6}$$

$$k_{SP} = 2\pi f\sqrt{T\rho(\lambda)C(\lambda)} \tag{7}$$

with

$$\rho(\lambda) = \frac{\rho_{air}}{GS(\lambda)} \tag{8}$$

$$GS(\lambda) = 1 - \frac{\tanh\left(\lambda\sqrt{-i}\right)}{\lambda\sqrt{-i}} \tag{9}$$

$$\lambda = \sqrt{\frac{6\rho_{air}\pi f T}{\varphi\sigma}} \tag{10}$$

$$C(\lambda) = \frac{1}{\gamma P_0}\left[\gamma - (\gamma-1)G_S\left(\lambda\sqrt{N_{PR}}\right)\right] \tag{11}$$

In these equations, P_0 is the isothermal bulk modulus of air (=142 kPa), γ the adiabatic constant (=1.4) and N_{pr} the Prandtl number of air (=0.713). T is the tortuosity of the medium, whose value can be calculated by assuming the same relationship with the medium porosity as expressed by Eq. (5):

$$T = \sqrt{\frac{1}{\varphi}} \tag{12}$$

The one-parameter physically inadmissible [37] Delany and Bazley (DB) model [38] is considered as well in this work, although it is unlikely that good model fits will be obtained. It is nevertheless added for illustrative purposes, since this model is still widely used in many outdoor sound propagation applications, and engineering methods (see e.g. [2,3]) provide forest floor flow resistivity values for this model:

$$X = \sqrt{\frac{f\rho_{air}}{\sigma}} \tag{13}$$

$$Z_{c,DB} = 1 + 0.0571X^{-0.754} + i0.087X^{-0.732} \tag{14}$$

$$k_{DB} = \left(\frac{2\pi f}{c}\right)\left(1 + 0.0978X^{-0.700} + i0.189X^{-0.595}\right) \tag{15}$$

All impedance models are considered in a (locally reacting) rigid-backing configuration. In general, it was found in [14] that this approach increases the accuracy of the fitting on outdoor grounds. It can thus be reasonably expected that this approach will be beneficial as well for a forest floor, given that the mineral layer is a medium with a much higher characteristic impedance than the upper layers of the forest floor (see e.g. [12] for evidence on this). The surface impedance Z_s can then be calculated based on the respective characteristic impedance $Z_{c,ground}$ and wave number in the ground medium k_{ground}:

$$Z_s = iZ_{c,ground}\cot\left(k_{ground}d\right) \tag{16}$$

where d is the layer thickness of the rigid backing model.

2.2.5. Non-acoustical soil properties

Four non-acoustical variables were determined to characterize the organic forest floor and topsoil layers: mineral soil bulk density, the gravimetric soil water content, the dry weight of the organic forest floor layer, and its water content. The mineral soil bulk density and the soil water content of the topsoil were determined using so-called Kopecky rings with a fixed volume of 100 cm^3. Four samples were taken in each 4 m^2 plot, weighed and then dried in an oven at 105–110 °C for 24 h. After drying the samples were weighed again and the bulk density and soil water content determined, by dividing the dry weight in g by 100 cm^3 (g cm^{-3}) and by dividing the difference between the wet and the dry weight by the dry weight (g_{water} per $g_{dry\ soil}$). The biomass of the forest floor layer was determined by collecting all organic material in a 20 cm × 20 cm square at three random locations around the 4 m^2 area defined by the metal frame (see Section 2.2.2). After drying the material at 65 °C during 24 h the dry mass (g m^{-2}) and the water content (g_{water} per $g_{dry\ litter}$) were determined. All measurements mentioned were conducted in summer and in winter.

2.2.6. In-situ measurement sequence

After assembling the measurement frame and performing microphone calibration, a first measurement was made above the undisturbed forest floor, for the 0.2 m and 0.5 m microphone

height pair. Next, the measurement was performed for the 0.2 m and 0.75 m microphone height pair. Then, the frame was rotated over 90° and the measurements for both height pairs were repeated.

In a next step, the entire organic forest floor layer was removed (by raking away) in the 4 m^2 square defined by the measurement frame, exposing the top of the mineral soil. The four acoustical measurements (see previous paragraph) were then repeated. Afterwards, soil samples (see Section 2.2.5) were gathered.

2.3. Statistical analysis

Statistical analysis of the performance of the ground impedance models to approach the spectral level difference measurements is performed with analysis of variance (ANOVA). A three-way ANOVA with independent variables tree species, season and organic layer presence (or absence), allowing for full interactions, is considered. One-way ANOVA is used for analyzing a subset of the data, followed by post-hoc tests (Tukey-Kramer) to determine which means are significantly different.

A paired-samples *t*-test was used to compare the deduced acoustical ground parameters at a first positioning of the source-receiver containing frame, and after rotating over 90°, at the same spot. Variability of the acoustical ground properties in the monoculture plots is analyzed with Bartlett's test for equal variances.

Next, a General Linear Model (GLM) was used to analyze the treatment effects on the deduced surface impedance, thereby adopting the MANOVA method for analyzing repeated measures designs [39]. In our model, tree species was the between-subject effect, whereas litter removal (yes versus no) was the within-subject effect. We opted to run separate analyses for the summer and winter measurements since the soil water content was three times higher in winter (0.42 ± 0.07) than in summer (0.14 ± 0.06), which is expected to have a large impact on the impedance.

Finally, linear regression is used to find dependencies between the non-acoustical and acoustical forest floor properties. Only undisturbed forest floors are considered in this analysis as this represents the true situation in the field. Given the strong differences in the non-acoustical properties between summer and winter conditions, separate regressions are made. Only regression models with parameters that are significant at the 5% significance level will be retained.

All analyses were performed with the Matlab's (R2019b) statistical toolbox and IBM's SPSS Statistics 26.

3. Results and discussion

3.1. Ground parameters deduction

Given that the loudspeaker and microphones have finite dimensions, preliminary measurements were made in a semi-anechoic chamber to find the source and receiver heights, and their separations, for best use with the analytical point source-point receiver model described in Section 2.2.3. A description of these supporting measurements is found in Appendix A.

Using this optimized source-receiver geometry, the impedance model parameters were deduced from the *in-situ* measurements above the undisturbed forest floor (see Fig. 2b) and presented in Table 1 (winter data) and Table 2 (summer data). Similar tables for the bare mineral soil can be found in Appendix B. The two microphone height pairs were simultaneously considered during the fitting procedure on the measurements, with an equal weight for each 1/3 octave band in the range from 100 Hz to 2500 Hz on condition that there is a signal-to-noise ratio of at least 10 dB.

A brute-force optimization was performed, running over all parameter combinations, and only slowly reducing the search intervals on the parameters when going to the next iteration. The search ranges for flow resisitivity were between 1 and 400 kPas/m^2, for porosity between 0.01 and 1.00, and for layer thickness between 0.001 and 0.2 m. The goal was minimizing the root-mean-square error (RMSE) between the measured and modeled spectral level differences. Although such a brute-force approach might be (computationally) less efficient, it reduces the risk of ending up with a set of ground impedance parameters that did not lead to the smallest possible fitting error (the so-called "local optimum" problem).

As shown in Tables 1 and 2, the SP and the ZK ground impedance models, both in rigid-backing, give very similar fitting errors overall. Therefore, only the soil parameters obtained from one of these impedance models (namely the ZK model) will be further analyzed. All deduced impedance spectra, separately for the summer and winter campaign, and both for the undisturbed forest floor as well as for the exposed mineral soil, are shown in Fig. 3. The rather constant real part of the surface impedance, and the strongly decreasing imaginary part with increasing frequency, is consistent with the measurements at forest floors reported e.g. in Ref. [12].

In the parameter range of interest, decreasing flow resistivity, increasing porosity and increasing layer thickness generally lead to a destructive ground interference becoming deeper and shifting to lower sound frequencies. For a more condensed analysis, the absolute value of the ground impedance (relative to the one of air) at 100 Hz was calculated with the best fitted parameters for each measurement.

The DB impedance model, in contrast, does not seem to be suited to model sound propagation over forest floors given the high overall fitting errors. Although represented in Tables 1 and 2, their use in outdoor sound propagation calculations should be discouraged, and this model is excluded from further analyses in this work.

The results of the non-acoustical characterization of the organic forest floor layer and (mineral) soil layer near the location of the measurement (see Section 2.2.5) is provided as well in Tables 1 and 2.

3.2. Impedance model performance

With the Delany and Bazley impedance model, an average root-mean-square-error (see Fig. 4) of 3.16 dB (winter campaign) and 3.33 dB (summer campaign) is obtained. This model, even in a rigid backing configuration, fails in predicting sound propagation over (undisturbed) forest floors, although this model is widely used as a general outdoor ground impedance model, including for this type of soil. These findings are in line with earlier observations and analyses [1,14,37].

The SP and ZK model, both in a rigid backing configuration, give much lower average fitting errors of 1.34 dB and 1.32 dB, respectively, during the winter campaign, and 0.94 dB and 0.99 dB, respectively, during the summer campaign at undisturbed forest floors. These models are thus able to capture the physical interactions between sound waves and forest floors reasonably well. Given their very similar performance, further analysis is performed with the ZK model only.

A three-way full-interaction ANOVA (with RMSE as dependent variable, and with season, species and presence/absence of the organic layer as independent variables) shows that especially season ($F_{1,92} = 61.59$, $p < 0.001$), but also species ($F_{5,92} = 3.14$, $p = 0.01$), are responsible for the observed variance in fitting error. Species and season do interact ($F_{5,92} = 2.57$; $p = 0.03$). During the winter campaign, the fitting error is significantly higher. The main difference between the summer and winter period is the much higher

Table 1
Overview of the winter measurement campaign data, showing the non-acoustically determined ground parameters, the fitting errors with the three impedance models considered, and the DB, SP and ZK effective soil parameters resulting in the best fit on the measured level differences. In addition, the relative impedance (i.e. the absolute value of the impedance, relative to the impedance of air) at 100 Hz is shown, using the best fitted parameters. Note that a fixed relation between the structure factor/tortuosity and porosity has been assumed for the ZK (Eq. (5)) and SP (Eq. (12)) models. The measurements above the undisturbed forest floor are provided here, so including the organic layer.

							RMSE (dB)			Delany and Bazley parameters			Slit pore soil parameters				Zwikker and Kosten soil parameters *			
	location ID	species	Soil bulk density (kg/m^3)	Soil gravimetric water content (kg/kg)	Litter dry weight (kg/m^2)	Litter gravimetric water content (kg/kg)	Delany and Bazley	Slit pore	Zwikker and Kosten	Flow resistivity (Pa s/m^2)	Layer thickness (m)	Relative impedance at 100 Hz	Flow resistivity (Pa s/m^2)	Porosity	Layer thickness (m)	Relative impedance at 100 Hz	Flow resistivity (Pa s/m^2)	Porosity	Layer thickness (m)	Relative impedance at 100 Hz
winter	1a1	Fraxinus	1088	0.36	0.66	2.83	2.30	1.47	1.47	219,230	0.014	31.60	65,920	0.56	0.031	32.4	69,240	0.51	0.032	33.0
	1a1-90	americana					2.88	1.58	1.57	63,530	0.015	29.51	119,720	1.00	0.038	15.3	124,100	1.00	0.037	15.2
	1a2	(ash)	940	0.54	0.52	3.42	2.23	1.26	1.26	33,890	0.015	28.79	76,080	0.63	0.032	27.5	74,170	0.56	0.034	28.2
	1a2-90						2.63	1.62	1.45	1000	0.018	26.96	48,520	0.41	0.046	29.3	46,100	0.34	0.050	32.0
	5a1	Tilia cordata	1177	0.35	0.55	2.59	1.70	1.54	1.53	90,960	0.008	53.92	185,800	0.90	0.013	46.1	192,380	0.87	0.013	46.5
	5a1-90	(lime)					2.16	1.61	1.58	73,450	0.008	54.75	181,970	1.00	0.093	15.1	189,170	1.00	0.089	15.2
	5a2		988	0.41	0.84	3.62	3.41	1.34	1.26	1000	0.018	27.79	51,470	0.36	0.057	27.5	53,710	0.32	0.057	29.2
	5a2-90						3.19	1.30	1.22	31,430	0.004	123.56	66,660	0.41	0.074	18.9	59,690	0.34	0.078	20.9
	5c1	Prunus avium	1041	0.38	0.63	1.50	3.53	1.68	1.71	1000	0.019	26.00	56,560	0.74	0.044	17.3	56,960	0.69	0.045	17.5
	5c1-90	(cherry)					4.00	1.24	1.19	66,290	0.008	54.38	53,520	0.50	0.085	13.5	44,280	0.41	0.101	13.6
	5c2		995	0.38	1.07	2.29	3.72	1.08	1.08	1000	0.018	27.64	57,490	0.61	0.067	13.9	53,640	0.53	0.071	14.6
	5c2-90						3.14	0.90	0.90	17,880	0.016	27.42	70,020	0.91	0.130	9.3	62,860	0.78	0.142	9.3
	6a1	Quercus rubra	1023	0.38	1.12	2.53	3.92	1.45	1.36	37,560	0.004	114.06	38,490	0.37	0.093	16.3	38,060	0.31	0.094	18.3
	6a1-90	(oak)					4.03	1.17	1.17	1000	0.018	27.27	49,110	0.46	0.077	15.9	46,830	0.41	0.082	16.6
	6a2		868	0.46	1.60	1.84	3.44	0.99	0.98	1000	0.017	28.20	61,790	0.73	0.087	10.0	53,290	0.61	0.102	10.0
	6a2-90						4.00	1.36	1.38	1000	0.019	26.42	32,130	0.60	0.142	7.7	30,430	0.53	0.142	8.1
	6c1	Fagus sylvatica	987	0.57	1.21	2.45	3.19	1.53	1.37	400,000	0.025	17.62	26,270	0.48	0.066	17.5	26,130	0.39	0.071	19.4
	6c1-90	(beech)					3.70	1.97	1.93	400,000	0.025	17.58	33,740	0.51	0.064	17.1	30,750	0.40	0.073	18.3
	6c2		980	0.46	1.60	2.83	3.39	0.98	1.01	400,000	0.145	3.03	24,200	0.43	0.098	13.3	24,730	0.37	0.102	14.5
	6c2-90						3.31	1.23	1.13	400,000	0.038	11.64	19,910	0.50	0.083	13.2	22,030	0.46	0.083	14.1
	8a1	Acer	975	0.40	0.49	3.45	2.94	1.11	1.14	400,000	0.038	11.62	29,000	0.73	0.068	11.3	27,660	0.64	0.074	11.6
	8a1-90	pseudoplatanus					2.94	1.19	1.21	400,000	0.025	17.53	34,910	0.65	0.056	15.2	35,070	0.59	0.060	15.6
	8a2	(maple)	910	0.42	0.56	3.40	3.15	1.31	1.31	51,400	0.015	29.57	112,780	0.92	0.040	15.8	107,080	0.84	0.042	16.0
	8a2-90						2.97	1.35	1.34	1000	0.018	27.10	59,230	0.59	0.044	21.5	56,340	0.51	0.048	22.2

Table 2
See caption of Table 1, but now for the summer measurement campaign.

							RMSE (dB)			Delany and Bazley parameters			Slit pore soil parameters				Zwikker and Kosten soil parameters *			
	location ID	species	Soil bulk density (kg/m^3)	Soil gravimetric water content (kg/kg)	Litter dry weight (kg/m^2)	Litter gravimetric water content (kg/kg)	Delany and Bazley	Slit pore	Zwikker and Kosten	Flow resistivity (Pa s/m^2)	Layer thickness (m)	Relative impedance at 100 Hz	Flow resistivity (Pa s/m2)	Porosity	Layer thickness (m)	Relative impedance at 100 Hz	Flow resistivity (Pa s/m2)	Porosity	Layer thickness (m)	Relative impedance at 100 Hz
summer	1a1	Fraxinus americana (ash)	858	0.11	0.45	0.06	2.69	0.71	0.71	42,540	0.017	25.7	83,930	0.78	0.036	20.0	77,300	0.71	0.040	19.3
	1a1-90						3.80	0.84	0.83	11,160	0.004	103.3	51,830	0.48	0.085	14.1	47,440	0.42	0.089	14.6
	1a2		728	0.10	0.50	0.11	3.51	1.31	1.36	2380	0.029	16.4	41,340	0.75	0.063	11.9	39,090	0.71	0.069	11.3
	1a2-90						3.12	1.25	1.27	400,000	0.145	3.0	31,260	0.63	0.103	9.0	27,590	0.57	0.119	8.5
	1a3		647	0.14	0.48	0.11	3.00	0.85	1.00	400,000	0.145	3.0	31,830	0.62	0.124	8.0	31,220	0.57	0.117	8.8
	1a3-90						4.06	0.62	0.62	34,720	0.018	25.3	45,280	0.65	0.087	10.5	40,260	0.58	0.096	10.4
	5a1	Tilia cordata (lime)	891	0.10	0.42	0.08	3.14	1.11	1.16	168,290	0.026	16.6	37,330	0.66	0.058	14.5	35,940	0.62	0.063	14.0
	5a1-90						3.65	1.06	1.09	168,290	0.026	16.6	30,990	0.57	0.073	13.3	29,570	0.52	0.079	13.3
	5a2		989	0.10	0.49	0.19	3.23	0.98	0.98	203,310	0.027	16.3	31,490	0.62	0.066	13.7	30,040	0.56	0.071	13.6
	5a2-90						3.47	1.40	1.41	2220	0.028	16.9	49,710	0.93	0.142	7.6	44,220	0.84	0.142	7.3
	5a3		1136	0.08	0.33	0.06	2.82	1.07	1.06	2170	0.029	16.7	50,410	0.76	0.047	15.8	45,590	0.67	0.053	15.4
	5a3-90						3.22	1.23	1.27	203,310	0.027	16.4	37,520	0.74	0.060	12.6	35,580	0.69	0.066	12.1
	5c1	Prunus avium (cherry)	903	0.12	0.92	0.09	3.84	0.71	0.74	1000	0.019	26.0	47,750	0.62	0.142	8.9	42,950	0.55	0.142	8.8
	5c1-90						3.32	1.01	1.00	138,640	0.009	50.9	109,900	0.82	0.043	16.4	92,340	0.70	0.051	15.8
	5c2		881	0.08	0.57	0.10	2.64	1.03	1.02	59,030	0.005	95.0	172,920	0.81	0.045	16.9	141,030	0.67	0.055	16.4
	5c2-90						3.19	1.25	1.25	28,510	0.005	98.3	82,550	0.55	0.124	12.5	70,420	0.48	0.141	12.1
	6a1	Quercus rubra (oak)	810	0.10	1.06	0.14	3.53	0.91	1.01	400,000	0.040	11.1	27,740	0.63	0.081	10.9	26,650	0.59	0.088	10.6
	6a1-90						2.38	0.80	0.90	400,000	0.145	3.0	25,020	0.72	0.089	8.9	23,800	0.67	0.096	8.6
	6a2		924	0.09	1.32	0.11	2.57	0.76	0.90	400,000	0.145	3.0	21,540	0.60	0.091	10.2	21,440	0.57	0.098	9.9
	6a2-90						2.49	0.63	0.73	400,000	0.145	3.0	25,880	0.64	0.109	8.2	24,200	0.59	0.118	8.1
	6a3		973	0.11	0.96	0.12	3.70	0.91	0.99	400,000	0.026	17.0	32,190	0.74	0.078	9.9	30,100	0.69	0.086	9.4
	6a3-90						3.45	1.23	1.33	203,310	0.026	16.6	31,720	0.59	0.068	13.9	31,310	0.56	0.073	13.4
	6c1	Fagus sylvatica (beech)	1263	0.21	0.84	0.24	3.41	0.72	0.76	63,980	0.017	25.6	61,600	0.62	0.054	17.0	57,290	0.57	0.059	16.5
	6c1-90						3.63	0.67	0.69	2190	0.029	16.8	47,830	0.61	0.060	15.4	44,370	0.56	0.066	15.0
	6c2		1030	0.16	1.34	0.21	3.43	0.99	1.05	31,770	0.017	26.1	67,540	0.55	0.052	19.5	64,880	0.52	0.056	18.7
	6c2-90						3.20	1.22	1.24	32,050	0.016	27.2	92,150	0.66	0.042	20.0	68,520	0.62	0.142	10.8
	6c3		1111	0.31	1.94	0.41	3.33	1.00	1.10	400,000	0.145	3.0	22,570	0.49	0.102	11.3	22,310	0.45	0.111	10.8
	6c3-90						3.61	0.66	0.96	400,000	0.040	11.0	21,270	0.47	0.083	14.2	23,370	0.45	0.087	13.9
	8a1	Acer pseudoplatanus (maple)	609	0.16	0.46	0.09	3.88	1.09	1.24	2190	0.029	16.8	40,620	0.71	0.142	7.6	43,150	0.55	0.075	13.4
	8a1-90						4.16	0.68	0.72	1000	0.019	25.5	36,060	0.60	0.142	8.0	33,500	0.55	0.142	8.1
	8a2		528	0.22	0.82	0.09	2.93	0.97	1.01	400,000	0.145	3.0	36,160	0.75	0.079	9.7	33,050	0.70	0.088	9.2
	8a2-90						3.44	0.90	0.98	400,000	0.041	10.7	26,380	0.64	0.084	10.4	25,210	0.59	0.091	10.1
	8a3		768	0.14	0.79	0.06	3.34	0.71	0.71	13,820	0.018	25.2	61,100	0.94	0.094	8.3	52,990	0.83	0.107	8.1
	8a3-90						3.38	0.56	0.55	20,760	0.017	25.9	67,950	0.84	0.08	9.4	58,340	0.74	0.098	9.2

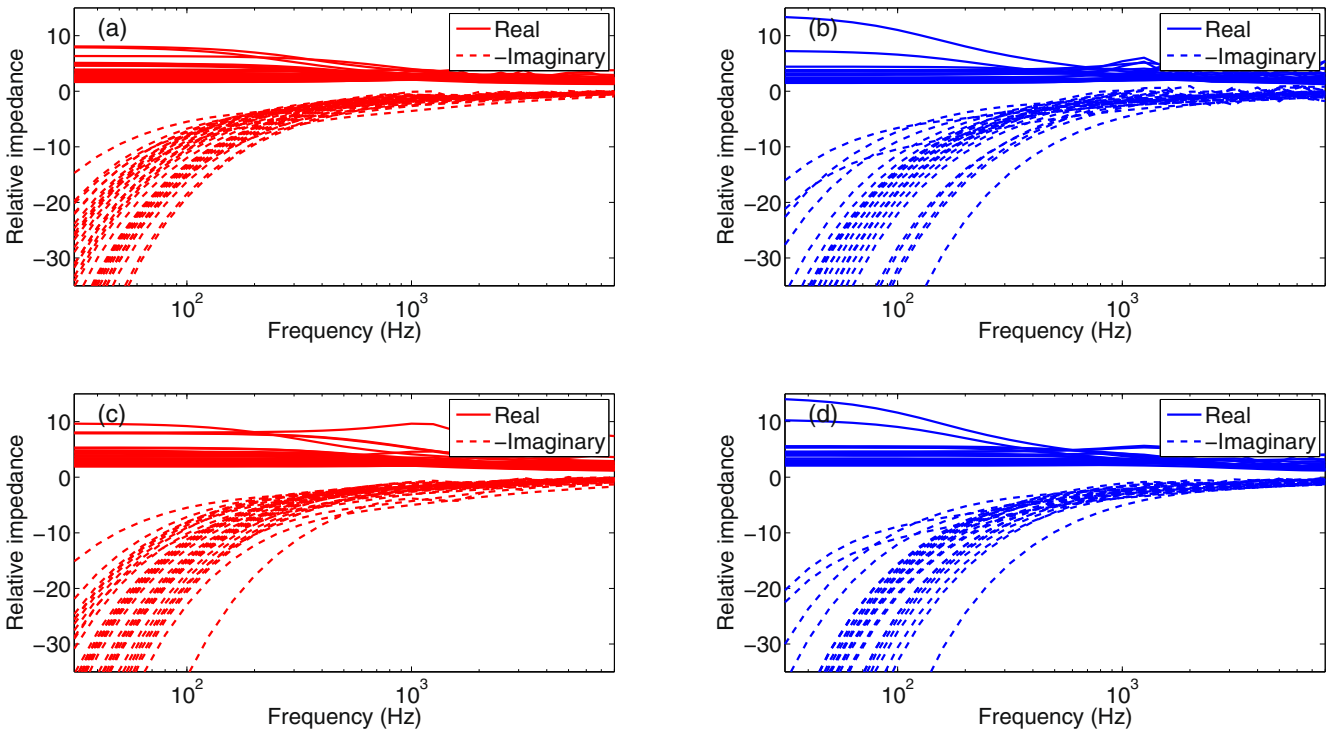

Fig. 3. Real and (negative) imaginary parts of the impedance spectra using the best fitted parameters for the Zwikker and Kosten model, for all forest floors considered. In (a) and (c), the summer measurements are shown (34 measurements), in (b) and (d), the winter measurements (24 measurements). In (a) and (b), the measurements above the undisturbed forest floor are shown, in (c) and (d) after removal of the organic forest floor layer.

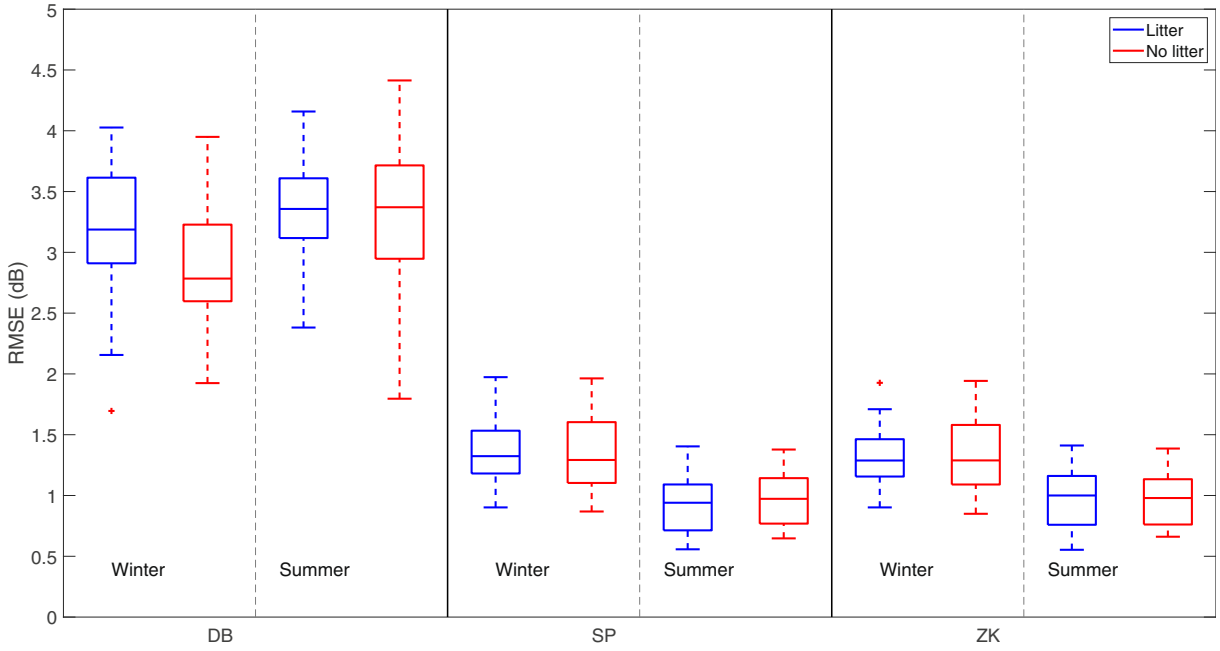

Fig. 4. Distributions of the RMSE of fitting the predicted level differences using the analytical propagation model on the measured data. All forest floor measurements, separately for the winter and summer campaign, in presence (="litter") and absence (="no litter") of the organic forest floor, are considered, for the three selected ground impedance models (DB = Delany and Bazley model, SP = slit-pore model, ZK = Zwikker and Kosten model). The (middle) horizontal lines in the boxes indicate the medians of the data. The boxes are closed by the first and third quartiles. The whiskers extend to at maximum 1.5 times the interquartile distance above the maximum values inside each box, and to at maximum 1.5 times the interquartile distance below the minimum values inside each box. Data points that fall outside these limits are indicated with the plus-signs.

water content in the mineral soil and organic forest floor layer (see Tables 1 and 2). The other non-acoustical properties of the mineral soil and organic forest floor, including the litter biomass, were not significantly different between summer and winter. This finding regarding modelling accuracy is consistent with literature reporting that larger water contents in the soil complicate ground surface impedance predictions [22,23]. The modeling performance above undisturbed forest floor and bare mineral soil is not at all

statistically significantly different ($F_{1,92} < 0.001$, $p = 0.98$). Note that in both situations, the rigid backing approach was followed for the surface impedance modeling.

When selecting for winter measurements only (including both presence and absence of the organic forest floor layer, and performing a one-way ANOVA), no significant differences in RMSE between species at the 5% significance level is found in a post-hoc Tukey-Kramer test. For the summer data only, ash and maple forest floors give statistically significantly lower fitting errors than lime.

In conclusion, the use of the SP and ZK impedance model, in a rigid backing configuration, is considered to be adequate. Possible hypotheses for its suitability under dry conditions is its ability to capture the transition between the organic top layer and the denser mineral soil, or to capture a densification of the mineral soil with depth for measurement when the mineral soil was exposed. Under wet conditions, the rigid-backing approach seems to capture the transition between saturated and non-water saturated soil. Although increased modeling performance could potentially be achieved with more advanced (and potentially multi-layered) ground impedance models, the latter is considered beyond the scope of the current paper.

3.3. Spatial variation of surface impedance

Each measurement was repeated at the same location, but with the source-receiver containing frame rotated over 90°. A paired *t*-test between the corresponding measurements, including both summer and winter data, showed that there were no statistically significant differences in the means ($t_{26} = 1.48$, $p = 0.15$) of the absolute value of the relative impedance at 100 Hz for the undisturbed forest floors. For the measurements with the organic layer removed, an even stronger (local) repeatability is observed ($t_{28} = 0.24$, $p = 0.81$). Similar conclusions can be made for the fitted (effective) flow resistivities and porosities. This shows that the measurements are sufficiently reproducible, and that strong (very) local variations in the forest floor properties are absent. When building a generalized linear model to predict the surface impedance (see Section 3.4), the data from such repetitions were consequently averaged.

Within a plot of the same tree species, there can be quite some variation in the deduced acoustic impedances as clearly indicated by the interquartile differences in the boxplots presented in Fig. 5. When combining all data (both in presence and absence of the organic layer, and both for summer and winter measurements), there are statistically significant differences in variance between species ($\chi^2_5 = 27.9$, $p < 0.001$); the largest variations are found at the ash, lime and beech stands. The effect of season on the variability of the surface impedance (across all species and including both presence and absence of the organic layer) is also strong ($\chi^2_1 = 18.8$, $p < 0.001$). During the winter campaign, the variation within a plot is roughly double of that observed during summer time.

Presence or absence of the organic forest floor does not lead to statistically significant differences in variance of the impedance ($\chi^2_1 = 0.21$, $p = 0.65$) over all species and when pooling for both summer and winter data.

3.4. Surface impedance magnitude

When plotting the distributions of the deduced relative impedances at 100 Hz (see Fig. 5), some general tendencies can yet be observed. During the summer measurements, the relative impedances are generally lower than during the winter measurements (mean M = 11.9, standard deviation SD = 3.2; and M = 19.1, SD = 8.9, respectively). The presence of an undisturbed forest floor, i.e. including the organic layer, leads to lower impedances compared to the situation where the sound waves directly interact with the (bare) mineral soil, both in summer and winter (M = 14.6, SD = 5.7; and M = 21.4, SD = 8.2, respectively).

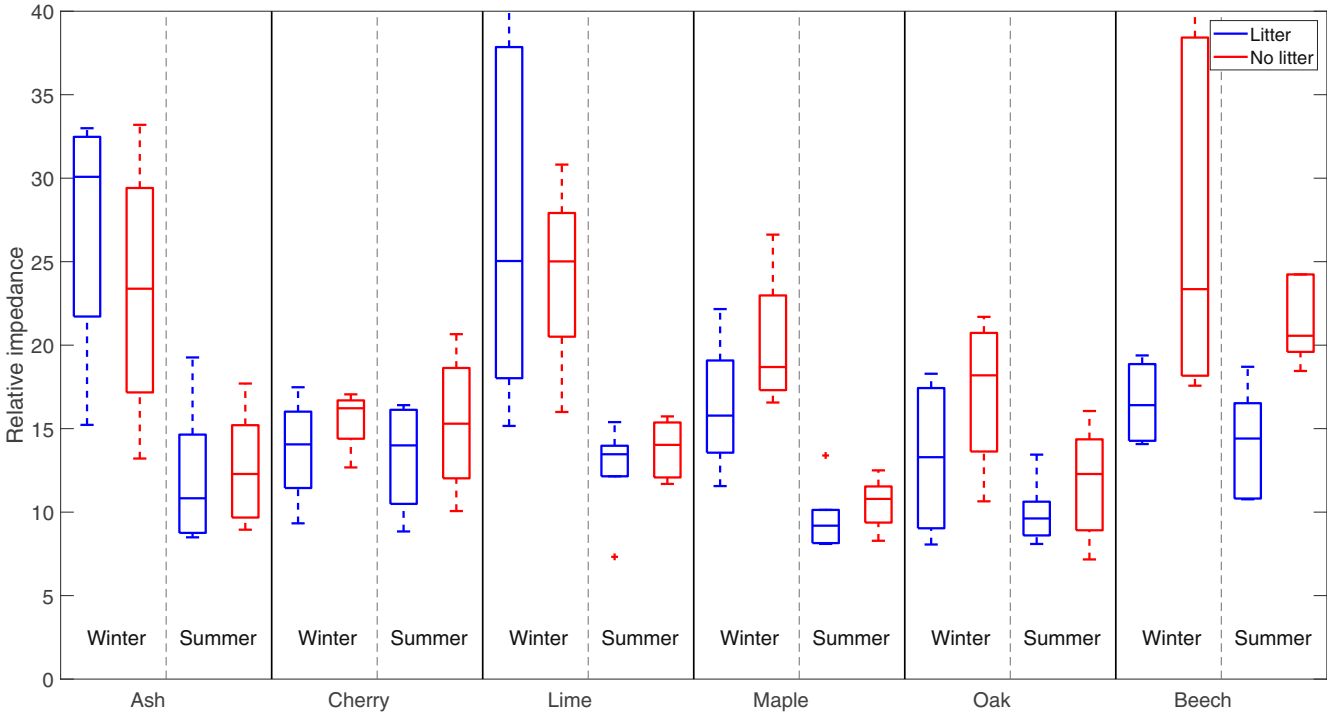

Fig. 5. Distributions of the deduced relative impedance at 100 Hz (ZK model), separately for species, season, and whether the organic forest floor was present or not.

Table 3
Results of repeated measures ANOVA analysis testing the effect of tree species identity and litter removal on the surface impedance magnitude.

	Summer	Winter
Between subjects effect		
Tree species	$F_{5,11}$ = 4.513; p = 0.018*	$F_{5,6}$ = 1.782; p = 0.251 ^{ns}
Within subjects effects		
Litter (yes/no)	$F_{1,11}$ = 12.709; p = 0.004**	$F_{1,6}$ = 2.204; p = 0.188 ^{ns}
Litter × Tree species	$F_{5,11}$ = 3.563; p = 0.037*	$F_{5,6}$ = 2.336; p = 0.166 ^{ns}

The repeated measures ANOVA (see Table 3) provides some deeper insights regarding what influences the surface impedance magnitude. Litter removal was only statistically significant during the summer period and interacted with tree species. No significant differences between species were found when the organic forest floor was present, suggesting that litter degradation speed alone is not a decisive parameter for its surface impedance magnitude in these developing forest floors. In contrast, a clear species-effect was found when the organic layer was removed. In the latter case, the impedance of beech, in particular, strongly increased and differed significantly ($p < 0.05$) from ash, maple and oak. During winter, no species, nor litter removal effects were found.

Linear regression analysis between the non-acoustical parameters considered and surface impedance leads to a few statistically significant models, but only with a limited predictive power. Soil bulk density, e.g., is negatively correlated with the impedance during summer ($r = 0.44$, $p = 0.008$). Using winter data only, more litter dry weight leads to a lower impedance ($r = 0.45$, $p = 0.026$). But a similar relationship between litter dry weight and impedance is not at all found when analyzing the summer measurements. So it seems that the interaction between sound waves and the forest floor is much more complicated than can be captured by such statistical inference. The use of these non-acoustical forest floor characterizations, common in forest ecological research, do not allow for meaningful predictions of the acoustical behavior.

4. Conclusions

The forest floor surface impedance, deduced from short range spectral level difference measurements using the template method, can be well approached by both the slit-pore and Zwikker and Kosten impedance model. These models, in a rigid backing configuration, adequately capture the physical interactions between sound waves and a variety of forest floor types. However, in case of larger moisture content, somewhat higher fitting errors were obtained.

At higher moisture contents, the forest floor surface impedance increases to a large extent. Another finding is that removal of the organic layer increased the forest floor surface impedance. However, a clear overall effect of tree species seems absent. Given that tree species has a strong impact on organic layer biomass consequently leads to the hypothesis that a thick organic layer might compensate for mineral soils that are acoustically harder. Indeed, a thick organic layer is linked to a low biological activity of soil macro-fauna and a less porous mineral layer. This is clearly seen at the beech stand, where raking away the organic layer strongly increased the surface impedance. When undisturbed, the surface impedance was of equal magnitude as the other species.

Note that the current measurements were performed in a relatively young forest, with the organic layers still in development. However, this could represent a realistic assessment of the forest floor effect when land is deliberately afforested for road traffic noise abatement.

Spatial variation of the surface impedance strongly depends on species and season. The variation within a plot during summer is roughly half at that during winter, although the somewhat larger fitting error during the wet winter measurements could play a role too. The largest variations are found in the ash, lime and beech stands. Very local variation is, however, not observed, giving confidence in the measurement methodology and processing.

When tree belts or forests are planned for noise reduction as an ecosystem service, litter removal should thus be discouraged. In addition, care is needed not to compact the mineral soil with machinery during maintenance or harvesting, especially in case of stands with more rapidly degrading litter. For these, the surface impedance strongly depends on the properties of the mineral layer.

CRediT authorship contribution statement

Timothy Van Renterghem: Conceptualization, Data curation, Formal analysis, Methodology, Validation, Visualization, Writing - original draft, Writing - review & editing. **Floris Huyghe:** Data curation, Formal analysis, Writing - review & editing. **Kris Verheyen:** Conceptualization, Writing - original draft, Writing - review & editing.

Declaration of Competing Interest

The authors declare that they have no known competing financial interests or personal relationships that could have appeared to influence the work reported in this paper.

Appendix A. Optimizing point source-receiver geometry in a semi-anechoic room

In a semi-anechoic room, the ground surface is known (i.e. fully rigid), allowing to optimize the point source height and (point) receiver heights, and their separation, for use with the analytical point source model (see Section 2.2.3). Test signals (see Section 2.2.2) were emitted several times at various positions inside the semi-anechoic room. The frame supporting the microphones and the loudspeaker was also assembled and disassembled multiple times to mimic field operation conditions.

Next, a so-called brute-force optimization was employed, where all combinations of the 5 unknown parameters (source height z_s, ground projected source-receiver separation y, and the 3 microphone heights $z_{r,1}$, $z_{r2,1}$ and $z_{r2,2}$) were simulated with the analytical model as discussed in Section 2.2.3 (with Q = 1). The search space was centered around the manually measured dimensions (y = 1.762 m, z_s = 0.510 m, $z_{r,1}$ = 0.185 m, $z_{r2,1}$ = 0.527 m, $z_{r2,2}$ = 0.728 m, RMSE = 2.1 dB), within a range of ± 10 cm on each parameter, in steps of 1 cm. The combination of dimensions yielding the lowest root-mean-square sound pressure level difference (=RMSE) with all measurements was consequently searched for. Each 1/3 octave band with centre frequencies from 100 Hz to 2.5 kHz was assigned an equal weight. Deviations between model and measurements at constructive and destructive interference dips will dominate the RMSE; this is actually interesting since such interferences are most sensitive to the exact geometry. The sound pressure level differences between the 50 cm and 20 cm microphone combination, and those for the 75 cm and 20 cm combination, were simultaneously optimized. Some slight deviations from the manually measured positions were found to be optimal (y = 1.682 m, z_s = 0.460 m, $z_{r,1}$ = 0.185 m, $z_{r2,1}$ = 0.577 m, $z_{r2,2}$ = 0.788 m), decreasing the RMSE to 1.6 dB.

The simulated and measured level differences in the semi-anechoic chamber are depicted in Fig. A1. A reasonably accurate modelling of the spectral level differences seems possible.

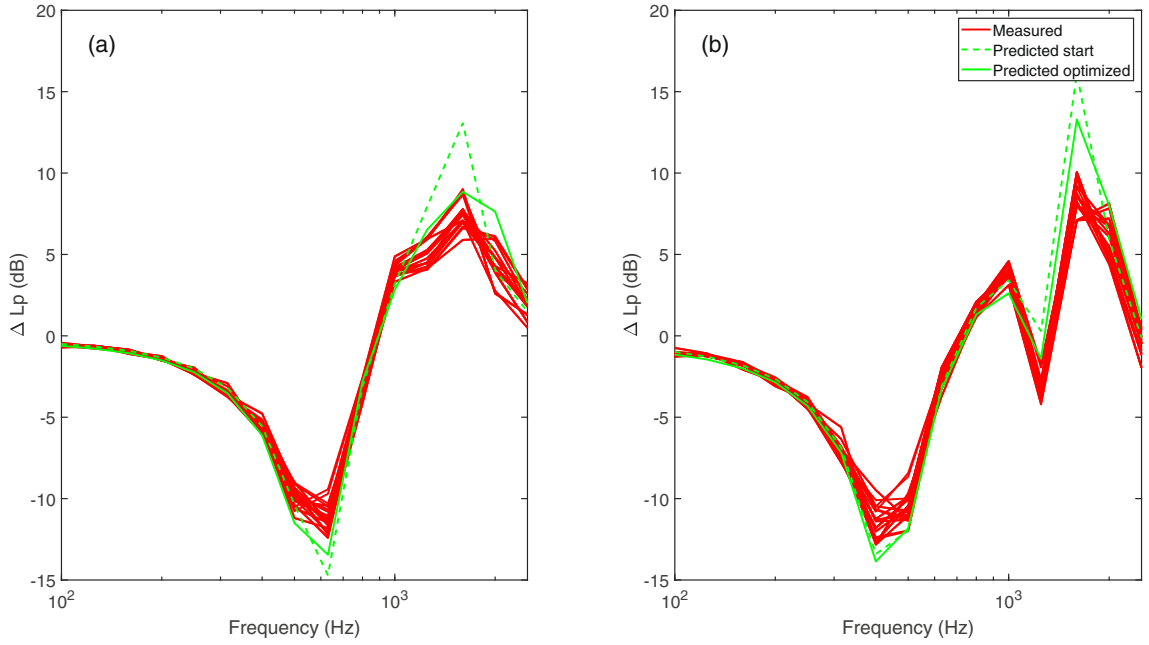

Fig. A1. Set of measured spectral sound pressure level differences between microphone height 50 cm and 20 cm (a), and between 75 cm and 20 cm (b). In addition, the simulated spectra using the manually measured dimensions (using the centre of the loudspeaker, and the centre of the microphone membrane, indicated as "Prediction start") are shown, together with the level difference spectra as a result of optimizing the dimensions of the setup by fitting on the data ("Predicted optimized"). The level differences are each time for the higher positioned microphone minus the lower positioned one.

Although measuring under well controlled conditions, there is still some variation in the exact values of the measured destructive and constructive interference dips and peaks upon repeating the measurements. In the forest, such very pronounced interferences do not appear, leading to overall smaller RMSE values (see Section 3). Another potential cause for uncertainty in the forest, not relevant in the semi-anechoic chamber, is that the surface will be irregular, and consequently, the ground plane might not be clearly defined. In addition, some scattering by the metal frame at higher frequencies cannot be fully excluded.

Appendix B. Fitting errors and deduced parameters for bare mineral soils

Tables B1 and B2.

Table B1
Overview of the winter measurement campaign data, showing the non-acoustically determined ground parameters of the bare mineral soil, the fitting errors with the three impedance models considered, and the DB, SP and ZK effective soil parameters resulting in the best fit on the measured level differences. In addition, the relative impedance (i.e. the absolute value of the impedance, relative to the impedance of air) at 100 Hz is shown, using the best fitted parameters. Note that a fixed relation between the structure factor/tortuosity and porosity has been assumed for the ZK (Eq. (5)) and SP (Eq. (12)) models. The measurements above the bare mineral soil are shown here, after raking away the organic top layer.

					RMSE (dB)			Delany and Bazley parameters			Slit pore soil parameters				Zwikker and Kosten soil parameters *			
	location ID	species	Soil bulk density (kg/m^3)	Soil gravimetric water content (kg/kg)	Delany and Bazley	Slit pore	Zwikker and Kosten	Flow resistivity (Pa s/m^2)	Layer thickness (m)	Relative impedance at 100 Hz	Flow resistivity (Pa s/m^2)	Porosity	Layer thickness (m)	Relative impedance at 100 Hz	Flow resistivity (Pa s/m^2)	Porosity	Layer thickness (m)	Relative impedance at 100 Hz
winter	1a1	Fraxinus	1088	0.36	2.59	1.26	1.25	25,420	0.016	28.7	124,620	1.00	0.027	21.0	130,240	1.00	0.026	21.1
	1a1-90	americana (ash)			2.97	1.96	1.94	22,140	0.010	45.1	136,890	1.00	0.048	13.1	142,030	1.00	0.047	13.2
	1a2		940	0.54	2.79	1.67	1.67	138,640	0.009	51.0	161,520	1.00	0.022	25.3	169,160	1.00	0.021	25.6
	1a2-90				2.67	1.62	1.58	1000	0.017	28.7	73,730	0.47	0.037	31.6	68,650	0.39	0.042	33.2
	5a1	Tilia cordata	1177	0.35	2.38	1.59	1.58	109,500	0.008	53.3	220,260	1.00	0.018	30.6	229,940	1.00	0.018	30.8
	5a1-90	(lime)			1.99	1.42	1.39	71,950	0.008	56.0	203,190	1.00	0.087	15.9	211,270	1.00	0.084	16.0
	5a2		988	0.41	2.87	1.25	1.23	109,150	0.003	131.5	92,500	0.36	0.063	25.1	83,208	0.33	0.067	25.0
	5a2-90				2.78	1.23	1.20	184,090	0.003	140.3	85,510	0.36	0.068	22.9	79,520	0.31	0.071	25.0
	5c1	Prunus avium	1041	0.38	3.59	1.19	1.20	1000	0.019	26.4	59,360	0.69	0.050	16.5	55,930	0.60	0.053	17.1
	5c1-90	(cherry)			3.23	1.05	1.02	35,850	0.005	96.9	65,150	0.48	0.076	16.0	56,760	0.40	0.086	16.1
	5c2		995	0.38	3.39	1.61	1.61	47,180	0.008	55.1	139,960	1.00	0.036	16.1	146,660	1.00	0.035	16.3
	5c2-90				2.77	0.98	0.98	138,640	0.009	51.5	136,240	1.00	0.093	12.6	142,550	1.00	0.089	12.7
	6a1	Quercus rubra	1023	0.38	2.61	1.05	1.03	138,640	0.009	51.2	179,120	1.00	0.026	21.5	186,240	1.00	0.026	21.7
	6a1-90	(oak)			2.71	1.33	1.33	21,730	0.004	100.5	224,680	1.00	0.030	19.4	235,580	1.00	0.029	19.8
	6a2		868	0.46	2.91	0.87	0.85	12,570	0.004	112.7	97,630	0.54	0.069	16.2	84,420	0.45	0.078	16.6
	6a2-90				3.60	1.18	1.18	1000	0.018	27.9	63,070	0.69	0.084	10.8	54,920	0.58	0.098	10.6
	6c1	Fagus sylvatica	987	0.57	2.67	1.85	1.84	38,090	0.009	48.8	170,470	1.00	0.020	27.6	178,340	1.00	0.020	27.9
	6c1-90	(beech)			1.92	1.57	1.56	67,810	0.008	58.4	248,840	0.93	0.012	48.2	248,750	0.88	0.013	48.9
	6c2		980	0.46	3.95	1.83	1.83	91,080	0.024	18.1	51,690	0.62	0.053	16.9	49,240	0.54	0.057	17.6
	6c2-90				2.22	0.91	0.91	1000	0.018	27.9	90,350	1.00	0.030	18.8	94,590	1.00	0.029	18.8
	8a1	Acer	975	0.40	3.88	1.45	1.41	91,080	0.025	17.9	43,510	0.58	0.062	15.6	39,610	0.48	0.069	16.6
	8a1-90	pseudoplatanus			3.20	1.15	1.15	187,390	0.023	18.9	50,530	0.61	0.049	18.8	49,080	0.54	0.052	19.3
	8a2	(maple)	910	0.42	3.22	1.33	1.33	39,030	0.015	29.1	125,930	0.99	0.032	17.7	117,100	0.88	0.035	18.0
	8a2-90				2.59	0.91	0.91	54,530	0.015	28.7	78,610	0.57	0.037	26.0	76,330	0.51	0.040	26.6

Table B2
See caption of Table B1, but now for the summer measurement campaign.

					RMSE (dB)			Delany and Bazley parameters			Slit pore soil parameters				Zwikker and Kosten soil parameters*			
	location ID	species	Soil bulk density (kg/m^3)	Soil gravimetric water content (kg/kg)	Delany and Bazley	Slit pore	Zwikker and Kosten	Flow resistivity (Pa s/m^2)	Layer thickness (m)	Relative impedance at 100 Hz	Flow resistivity (Pa s/m2)	Porosity	Layer thickness (m)	Relative impedance at 100 Hz	Flow resistivity (Pa s/m2)	Porosity	Layer thickness (m)	Relative impedance at 100 Hz
summer	1a1	Fraxinus americana (ash)	858	0.11	3.90	0.77	0.75	1000	0.019	25.6	57,100	0.53	0.072	14.9	51,200	0.47	0.078	15.2
	1a1-90				3.38	0.86	0.83	9020	0.004	107.8	57,060	0.42	0.082	16.6	52,620	0.36	0.085	17.7
	1a2		728	0.10	3.56	0.82	0.83	53,360	0.017	25.4	62,470	0.80	0.055	13.0	56,880	0.73	0.061	12.5
	1a2-90				4.41	1.31	1.30	1000	0.020	24.9	38,630	0.62	0.097	9.8	34,350	0.55	0.107	9.7
	1a3		647	0.14	4.33	0.80	0.84	1000	0.019	25.6	34,190	0.52	0.142	8.6	32,390	0.47	0.142	8.9
	1a3-90				3.97	0.71	0.69	31,080	0.017	25.7	53,800	0.62	0.077	12.1	47,340	0.54	0.086	12.0
	5a1	Tilia cordata (lime)	891	0.10	2.88	0.82	0.85	1000	0.029	16.9	44,600	0.67	0.051	16.3	42,370	0.62	0.056	15.7
	5a1-90				3.57	1.07	1.06	1000	0.029	16.7	34,470	0.55	0.070	14.6	32,800	0.49	0.075	14.8
	5a2		989	0.10	3.83	1.38	1.39	152,370	0.026	16.6	34,860	0.65	0.075	11.5	31,930	0.57	0.082	11.7
	5a2-90				3.52	1.36	1.36	28,130	0.017	25.9	82,470	0.93	0.045	13.8	75,210	0.85	0.050	13.3
	5a3		1136	0.08	2.86	1.13	1.13	1150	0.029	16.8	54,160	0.80	0.044	15.9	49,470	0.72	0.050	15.4
	5a3-90				3.36	1.18	1.20	187,390	0.027	16.4	40,270	0.74	0.061	12.4	37,440	0.68	0.067	12.1
	5c1	Prunus avium (cherry)	903	0.12	3.72	0.77	0.75	15,220	0.004	101.5	54,490	0.53	0.111	10.9	44,720	0.46	0.142	10.1
	5c1-90				2.96	0.98	0.98	138,640	0.009	51.6	165,670	1.00	0.034	17.2	153,350	0.94	0.037	16.6
	5c2		881	0.08	2.22	1.26	1.25	42,320	0.004	104.6	189,230	0.55	0.053	21.3	148,600	0.45	0.065	20.7
	5c2-90				2.83	1.20	1.20	25,170	0.004	100.0	100,750	0.51	0.121	14.3	86,030	0.44	0.138	14.0
	6a1	Quercus rubra (oak)	810	0.10	3.13	0.97	0.98	1000	0.029	17.1	54,600	0.89	0.051	12.6	50,900	0.83	0.055	12.1
	6a1-90				3.39	0.99	1.00	1000	0.028	17.3	47,430	0.91	0.142	7.5	41,560	0.81	0.142	7.2
	6a2		924	0.09	3.39	0.74	0.74	1020	0.028	17.4	56,870	0.85	0.052	12.9	51,360	0.77	0.058	12.5
	6a2-90				3.45	0.76	0.76	16,290	0.018	24.9	64,010	0.92	0.074	9.3	55,030	0.81	0.087	8.9
	6a3		973	0.11	2.91	1.14	1.15	1000	0.028	17.6	65,060	0.92	0.041	14.9	59,550	0.84	0.046	14.4
	6a3-90				3.00	1.09	1.09	103,060	0.018	25.0	70,340	0.84	0.040	16.7	65,060	0.78	0.044	16.1
	6c1	Fagus sylvatica (beech)	1263	0.21	2.62	0.72	0.72	1000	0.018	27.0	133,690	1.00	0.026	21.3	132,030	1.00	0.027	20.3
	6c1-90				3.16	0.76	0.76	1000	0.019	26.4	86,680	0.64	0.043	20.2	79,070	0.58	0.048	19.6
	6c2		1030	0.16	1.80	1.16	1.12	27,060	0.003	146.0	175,100	0.24	0.067	35.5	132,610	0.20	0.074	36.7
	6c2-90				1.85	1.08	1.08	20,590	0.004	100.7	408,340	1.00	0.024	25.0	402,990	1.00	0.024	24.2
	6c3		1111	0.31	3.28	1.02	1.02	1000	0.018	27.1	107,810	0.82	0.036	19.0	93,230	0.71	0.042	18.5
	6c3-90				2.95	1.20	1.20	1000	0.019	26.1	96,730	0.76	0.034	21.5	85,940	0.67	0.039	20.8
	8a1	Acer pseudoplatanus (maple)	609	0.16	3.93	0.65	0.66	1000	0.020	25.1	39,820	0.61	0.142	8.2	36,190	0.55	0.142	8.3
	8a1-90				3.91	0.81	0.81	31,870	0.005	96.6	42,260	0.53	0.136	9.3	38,120	0.47	0.142	9.4
	8a2		528	0.22	3.71	0.81	0.82	2320	0.028	17.1	54,080	0.77	0.062	11.9	48,690	0.70	0.070	11.5
	8a2-90				4.04	1.00	1.03	152,370	0.026	16.6	32,610	0.57	0.077	12.7	31,200	0.53	0.083	12.5
	8a3		768	0.14	3.16	0.80	0.79	17,430	0.017	26.5	91,350	1.00	0.062	10.4	90,080	1.00	0.063	10.2
	8a3-90				3.24	0.73	0.72	43,740	0.009	47.1	87,620	0.74	0.075	11.8	74,330	0.64	0.088	11.4

References

[1] Attenborough K, Van Renterghem T. Predicting outdoor sound. 2nd ed. Taylor and Francis Boca Raton-Oxon: CRC Press; 2021.
[2] Kragh J, Plovsing B. Nord2000: Comprehensive Outdoor Sound Propagation Model. Part I-II. DELTA Acoustics & Vibration Report, 1849–1851/00; 2000.
[3] Kephalopoulos S, Paviotti M, Anfosso-Lédée F. Master report on Common Noise Assessments Methods in Europe (CNOSSOS-EU) Outcome and Resolutions of the. CNOSSOS-EU Technical Committee & Working Groups; 2012.
[4] Attenborough K, Bashir I, Taherzadeh S. Exploiting ground effects for surface transport noise abatement. Noise Mapp 2016;3:1–25.
[5] Cook D, Van Haverbeke D. Trees and Shrubs for Noise Abatement, Research Bulletin 246, Historical materials from. University of Nebraska-Lincoln Extension, Paper; 1629; 1971.
[6] Aylor D. Noise reduction by vegetation and ground. J Acoust Soc Am 1972;51:197–205.
[7] Fricke F. Sound-attenuation in forests. J Sound Vib 1984;92:149–58.
[8] Huisman W, Attenborough K. Reverberation and attenuation in a pine forest. J Acoust Soc Am 1991;90:2664–77.
[9] Crocker M. Encyclopedia of acoustics. New York: John Wiley & Sons; 1997.
[10] Li M, Van Renterghem T, Kang J, Verheyen K, Botteldooren D. Sound absorption by tree bark. Appl Acoust 2020;165:107328.
[11] Van Renterghem T, Botteldooren D, Verheyen K. Road traffic noise shielding by vegetation belts of limited depth. J Sound Vib 2012;331:2404–25.
[12] Martens M, van der Heijden L, Walthaus H, van Rens W. Classification of soils based on acoustic impedance, air flow resistivity, and other physical soil parameters. J Acoust Soc Am 1985;78:970–80.
[13] Attenborough K. Review of ground effects on outdoor sound propagation from continuous broadband sources. Appl Acoust 1988;24:289–319.
[14] Attenborough K, Bashir I, Taherzadeh S. Outdoor ground impedance models. J Acoust Soc Am 2011;129:2806–19.
[15] Berg B, McClaugherty C. Plant litter : decomposition, humus formation, carbon sequestration. 4th ed. Switzerland: Springer Nature; 2020.
[16] Allard K, Atalla N. Propagation of sound in porous media: modelling sound absorbing materials. 2nd ed. John Wiley and sons; 2009.
[17] Schelfhout S, Mertens J, Verheyen K, Vesterdal L, Baeten L, Muys B, et al. Tree species identity shapes earthworm communities. Forests 2017;8:85.
[18] Ding L, Van Renterghem T, Botteldooren D, Horoshenkov K, Khan A. Sound absorption of porous substrates covered by foliage: experimental results and numerical predictions. J Acoust Soc Am 2013;134:4599–609.
[19] Connelly M, Hodgson M. Experimental investigation of the sound absorption characteristics of vegetated roofs. Build Environ 2015;92:335–46.
[20] Attal E, Dubus B, Leblois T, Cretin B. An optimal dimensioning method of a green wall structure for noise pollution reduction. Build Environ 2021;187:107362.
[21] Dickinson P, Doak P. Measurements of the normal acoustic impedance of ground surface. J Sound Vib 1970;13:309–22.
[22] Cramond A, Don C. Effect of moisture content on soil impedance. J Acoust Soc Am 1987;82:293–301.
[23] Horoshenkov K, Mohamed M. Experimental investigation of the effects of water saturation on the acoustic admittance of sandy soils. J Acoust Soc Am 2006;120:1910–21.
[24] Oshima T, Hiraguri Y, Okuzono Y. Distinct effects of moisture and air contents on acoustic properties of sandy soil. J Acoust Soc Am Express Lett 2015;138:EL258–63.
[25] Kurosaka Y, Oshima T, Honda M. Influence of weather on the acoustical properties of a ground surface: measurements and models. Noise Contr Eng J 2018;66:505–22.
[26] Briggs R. Soil development and properties | the forest floor. Encyclopedia For Sci 2004;1223–1227.
[27] Keith D, Johnson E, Valeo C. Moisture cycles of the forest floor organic layer (F and H layers) during drying. Water Resour Res 2010;46. W07529.
[28] Kalinina O, Chertov O, Frolov P, Goryachkin S, Kuner P, Küper J, et al. Alteration process during the post-agricultural restoration of Luvisols of the temperate broad-leaved forest in Russia. CATENA 2018;171:602–12.
[29] de Schrijver A, de Frenne P, Staelens J, Verstraeten G, Muys B, Vesterdal L, et al. Tree species traits cause divergence in soil acidification during four decades of post-agricultural forest development. Glob Change Biol 2012;18:1127–40.
[30] Guillaume G, Faure O, Gauvreau B, Junker F, Bérengier M, L'Hermite P. Estimation of impedance model input parameters from in situ measurements: Principles and applications. Appl Acoust 2015;95:27–36.
[31] Nordtest. NT-ACOU-104: Ground surfaces: Determination of the acoustic impedance. Espoo, Finland: Nordic innovation centre; 1999.
[32] ANSI/ASA S1.18-2018. Method For Determining The Acoustic Impedance Of Ground Surfaces; 2018.
[33] Zwikker C, Kosten C. Sound absorbing materials. New York: Elsevier; 1949.
[34] Van Renterghem T. Efficient outdoor sound propagation modeling with the finite-difference time-domain (FDTD) method: a review. Int J Aeroacoust 2014;13:385–404.
[35] Stinson M. The propagation of plane sound waves in narrow and wide circular tubes and generalisation to uniform tubes of arbitrary cross-sectional shape. J Acoust Soc Am 1991;89:550–8.
[36] Attenborough K. On the acoustic slow wave in rigid framed porous media. J Acoust Soc Am 1987;81:93–102.
[37] Dragna D, Attenborough K, Blanc-Benon P. On the inadvisability of using single parameter models for representing outdoor ground impedance. J Acoust Soc Am 2015;138:2399–413.
[38] Delany M, Bazley E. Acoustical properties of fibrous absorbent materials. Appl Acoust 1970;3:105–16.
[39] O' Brien R, Kaiser M. MANOVA Method for analyzing repeated measures designs: an extensive primer. Psychol Bull 1985;97:316–33.